Cancer Nanotechnology

RESEARCH Open Access

Hypobaric hypoxia exposure regulates tissue distribution of nanomedicine for enhanced cancer therapy

Ye Tao[1] and Zhongping Chen[2*]

*Correspondence:
chenzp@ntu.edu.cn

[1] Medical School, Nantong University, Nantong, People's Republic of China
[2] Institute of Special Environmental Medicine, Nantong University, Nantong, People's Republic of China

Abstract

Background: Effective drug delivery of nanomedicines to targeted sites remains challenging. Given that hypobaric hypoxia and hyperbaric oxygen exposure can significantly change pharmacokinetics of drugs, it is interesting to determine whether they can regulate tissue distribution of nanomedicine, especially in tumor, for enhanced cancer therapy.

Results: Hypobaric hypoxia exposure improved the pharmacokinetics of paclitaxel-loaded liposomes and facilitated their distribution in the heart and liver, whereas hyperbaric oxygen exposure did not benefit and even impaired the pharmacokinetics and distribution. Particularly, both hypobaric hypoxia and hyperbaric oxygen exposure could not improve the distribution in subcutaneous tumor. Thus, we constructed orthotopic liver tumor model and discussed whether high distribution of the liposomal nanomedicine in the liver, facilitated by hypobaric hypoxia exposure, could ensure their effective accumulation in liver tumor for enhanced cancer therapy.

Conclusions: The liposomal nanomedicine with adjuvant hypobaric hypoxia exposure significantly inhibited the growth of orthotopic liver tumor for prolonged survival time, achieved by hypobaric hypoxia-promoted accumulation at tumor sites of the liver. It might be the first example of the application of adjuvant intermittent hypobaric hypoxia exposure in treating liver cancer.

Keywords: Hypobaric hypoxia, Hyperbaric oxygen, Liposomes, Tissue distribution, Cancer therapy

Introduction

Nowadays, cancer is one of the leading causes of mortality all over the world, which remains a clinical challenge. Despite various treatment approaches developed, chemotherapy using toxic therapeutic agents is still the most utilized treatment regimen in clinic (Anand et al. 2023). Due to unsatisfactory pharmacokinetics and lack of specificity of therapeutic agents, therapeutic benefit of conventional chemotherapy is far from satisfactory, which is also accompanied by severe adverse effects. The past decades have witnessed great progress of nanomedicines for in vivo drug delivery for cancer therapy

(Behranvand et al. 2022). Nanomedicines using nanoparticles as carrier of therapeutic agents can not only significantly improve pharmacokinetics of therapeutic agents, facilitating their accumulation in tumor, but also reduce their toxicity to normal tissues and cells by shielding them (Bhatia et al. 2022). As a result, enhanced therapeutic outcome along with reduced adverse effects is predictable, as extensively validated in xenograft tumor model. On the other hand, clinical data from nanomedicines approved and still in clinical trials affirm that therapeutic outcome of nanomedicines is overrated and their outstanding benefit is reduced adverse effects for better life quality but not prolonged survival rate of cancer patients (Zhang et al. 2023). Thus, clinical translation of nanomedicines is largely impeded with approved nanomedicines far below expectations (Sun et al. 2022a).

Since first investigated by Matsumura and Maeda in 1986, the EPR effect, arising from defective tumor vasculature for drug accumulation and dysfunctional lymphatic systems for drug retention in tumor, becomes the rationale for nanomedicine design. TME in animal xenograft tumor model is homogenous, contributing to consistent EPR effect in preclinical study. In contrast, the EPR effect in cancer patients is heterogeneous and variable even in an individual cancer patient, affected by a wide range of factors, such as tumor pathology and tumor stage (Zi et al. 2022), resulting from highly heterogeneous human TME. Over-idealizing the EPR effect might mainly lead to translational failure of many well-designed nanomedicines. Therefore, several strategies are developed to augment the EPR effect. As TME is a physical barrier against drug delivery, one promising strategy is to utilize EPR-enhancing agents to remodel TME to facilitate drug accumulation and penetration in tumor, which has already been tested in clinical trials (Subhan et al. 2023). However, this field requires more studies to assess the EPR effect in cancer patients. Moreover, the biosafety of EPR-enhancing agents should be also taken into consideration. Another strategy is to modify nanomedicines with targeting and/or TME-responsive moieties components to enhance drug delivery. The former involves surface-engineered moieties targeting TME components and cancer cells for targeted drug accumulation at tumor sites, while the latter involves incorporated responsive moieties, enabling sensitive release at tumor sites in responding to TME for improved bioavailability (Liu et al. 2023; Long et al. 2021, 2020; Lu et al. 2022; Sun et al. 2022b). However, this strategy needs sophisticate chemical modification and is thus not an easily achievable approach.

Continuous endeavors are still being made to improve drug delivery. It is a conclusion that the intrinsic physicochemical properties of nanomedicines, such as size, surface charge, surface chemistry, and shape, can regulate their distribution for improved drug delivery to targeted tissues as well as tumor (Cai et al. 2023). The exact relationships between the physicochemical properties and distribution are unfortunately inconclusive, attributing to the interrelationships of the physicochemical properties (Chen et al. 2023). In some cases, the results are even contrary. For example, Yang et al. reported that positively charged LPs were prone to be distributed into the lung (Yang et al. 2013), whereas He et al. found that negatively charged polymeric micelles, regardless of size, preferred to be distributed into the lung (He et al. 2010). Thus, targeted delivery through physicochemical properties-tailoring strategy remains challenging. It is reported that HH, referred as to reduced ambient pressure under high-altitude exposure, can lead to

a series of physiological changes of the body, which may affect absorption, metabolism, and elimination of a drug for significantly changed pharmacokinetics. Thus, intermittent HH is used to improve the pharmacokinetics of some common drugs for enhanced bioactivity, while not causing HH-related tissue damages or (Burtscher et al. 2022; Zhu et al. 2022). Meanwhile, considering that TME is hypoxic, which might be categorized into normobaric hypoxia being of reduced oxygen fraction, HBO, as a clinical treatment choice for carbon monoxide poisoning, decompression sickness, and other ischemic and hypoxic diseases, has recently emerged as a novel treatment regimen for cancer. Through nearly 100% oxygen and elevated atmosphere pressure, typically 2–3 ATA, HBO can effectively increase oxygen dissolved in the plasma and thus increase oxygen transport to major tissues as well as tumor in a hemoglobin-independent manner. As a result, HBO enhances drug penetration across tumor as well as enhancing the sensitivity of cancer to radiotherapy and photodynamic therapy for better therapeutic outcome (Liu et al. 2021; Wang et al. 2023; Wu et al. 2018).

Encouraged by these findings, it is interesting to determine the effect of external oxygen conditions, such as HH and HBO, on in vivo biodistribution of nanomedicines, especially in tumor, with the aim to improve their therapeutic outcome. However, related work is barely reported. Herein, we synthesized PTX-LPs and then compared their tissue distribution under AO, HH, and HBO conditions in subcutaneous tumor xenograft model. The results showed that HH improved the distribution of PTX-LPs in the heart and liver, whereas HBO did not benefit and even impaired the distribution. Notably, there is no difference found in the distribution in subcutaneous tumor under AO, HH and HBO, although HH could significantly improve pharmacokinetics of PTX-LPs. Thus, we further constructed orthotopic liver tumor model, attempting to improve the accumulation in tumor for effective live cancer therapy through HH-promoted distribution in the liver.

Materials and methods

Chemical, cell, and animal

All lipids, including DOPC, Chol, and DSPE–PEG), were purchased from AVT (Shanghai) Pharmaceutical Tech Co., Ltd. PTX was obtained from J&K Scientific (Shanghai, China). The other main chemicals were from Sinopharm Chemical Reagent (Shanghai, China).

Mouse hepatoma cell line (H22) was gotten from the Institute of Biochemistry and Cell Biology (Shanghai, China). Cells were cultured in RPIM-1640 supplemented with 10% fetal bovine serum. BALB/c mice (6 weeks, female) were supplied by Animal Center of Nantong University.

LPs synthesis and characterization

Synthetic procedure

Blank LPs were synthesized by the thin-film evaporation and ultrasonic hydration method according to the previous work (Cao et al. 2019; Wang et al. 2014). In a typical experiment, DOPC, Chol, and DSPE–PEG (4:1:0.6, w/w, total 11.2 mg) were mixed in 3 mL of chloroform in a round-bottomed flask. The mixture was evaporated under vacuum to form thin lipid film. The film was then hydrated with 5 mL of PBS (pH = 7.4)

for 10 min at room temperature, followed by bath sonication for 5 min, to obtain homogeneous liposomal suspension. To synthesize PTX-LPs, hydrophobic PTX was mixed with the lipids in chloroform in a ratio of the lipids to PTX (5:1, w/w), which was then subjected to evaporation, hydration, and sonication. The obtained PTX-LPs were finally transferred to a dialysis bag (MWCO = 14,000) and dialyzed against PBS (pH = 7.4) for 3 h under magnetic stirring to remove unloaded PTX. Due to poor solubility of DTX in water, Tween 80 was added into the PBS (0.5%, v/v) to increase the solubility when being dialyzed.

Morphology, size, and surface charge

TEM (JEM-200EX, JEOL) was used to observe the LPs. Liposomal suspension dropped on a copper grid needed negative staining before TEM observation. DLS (Zetasizer ZS90, Malvern) was used to determine the hydrodynamic diameter and zeta potential of the LPs. At least triplicate measurements were performed.

Drug encapsulation efficiency and loading efficiency

HPLC (Waters) was utilized to quantitatively analyze PTX using the following HPLC conditions: C_{18} column; methanol/acetonitrile (35:65, v/v) as the mobile phase; 230 nm as the detection wavelength. Twenty microliters of free PTX in methanol were injected into HPLC for analysis and a standard curve was obtained by plotting peak area of PTX against its concentration (0.1–10 μg/mL). To determine the encapsulation efficiency (EE, %) and loading efficiency (LE, %) of PTX, 0.2 mL of PTX-LPs suspension was treated with 3 mL of methanol and then filtered with 0.22 μm filter to remove precipitates. Afterwards, methanol solution containing loaded PTX was collected for HPLC analysis. EE was defined as loaded PTX versus totally added PTX, while LE was defined as loaded PTX versus totally added lipids plus loaded PTX.

In vitro drug release

In a typical experiment, 1 mL of PTX-LPs suspension transferred into in a dialysis bag (MWCO = 14,000) was immersed in 30 mL of PBS (pH = 7.4) containing 0.5% Tween 80 (v/v) with gently magnetic stirring, which was maintained under HH and BHO for 1.5 h. In the following, 1 mL of PBS (pH = 7.4) containing released PTX was withdrawn for HPLC analysis. The PBS was preconditioned under HH and BHO overnight. The ratio of released PTX to loaded PTX was determined as in vitro release ratio. Samples placed in AO was considered as control group.

Animal experiments

Tumor modeling

Subcutaneous tumor xenograft model was constructed by subcutaneously injecting 0.1 mL of H22 cell suspension (2×10^7 cells/mL) into right flank of BALB/c mice. To construct orthotopic liver tumor model, the liver of BALB/c mice was surgically exposed and 10 μL of H22 cell suspension (1×10^8 cells/mL) was then injected into the liver. The would was sealed and sutured. The cell suspension was placed on ice before use.

HH and HBO protocols High-altitude exposure at an altitude of 5000 m (oxygen partial pressure, $PaO_2 = 12$ kPa) in a HH chamber was performed to mimic HH exposure. Similarly, a customized HBO chamber was used to generate HBO (2.5 ATA, 100% oxygen). Mice were placed in HH or HBO chamber for 1.5 h. For HBO, mice were slowly decompressed before being taken out from the chamber.

Pharmacokinetics and tissue distribution study Pharmacokinetics and tissue distribution were studied in healthy and subcutaneous tumor-bearing BALB/c mice, respectively. Mice were intravenously injected with free PTX and PTX-LPs (5 mg PTX/kg body weight) and immediately subjected to HH or HBO exposure for 1.5 h. Immediately after the exposure, mice were taken out the chambers and sacrificed to collect blood and some major tissues, including the heart, liver, spleen, lung, kidney, brain, large intestine, small intestine, stomach, and tumor. For blood samples, the samples were centrifuged at 3000 rpm for 10 min and were then treated with a mixture of chloroform and methanol (4:1, v/v). After removing precipitates through filtering, followed by rotary evaporation to get rid of the organic solution, the samples were redissolved in methanol for PTX determination by HPLC. For tissue samples, the samples were first homogenized and then treated with the mixture of chloroform and methanol to determine PTX. Subcutaneous tumor-bearing mice received drug injection at the 12th day of subcutaneous tumor modeling. A group maintained under AO were regarded as control group.

Therapeutic study

Therapeutic outcome was studied in orthotopic liver tumor-bearing mice. Beginning at the 12th day of orthotopic liver tumor modeling, mice were intravenously injected with PTX-LPs (5 mg PTX/kg body weight) and immediately subjected to HH or HBO exposure for 1.5 h. This injection exposure was repeated for three times every three days. Body weight of mice was monitored every two days and their survival situation was checked every day. When at least three mice were alive in each group, mice were sacrificed and the liver was collected for observation, weighing, and for therapeutic study. Liver weight index was defined as liver weight versus body weight. Meanwhile, blood was collected for hematologic study.

Statistical analysis

All data were presented as mean ± standard deviation (SD) or mean ± standard error of the mean (SEM). Unpaired Student's *t* test was used for two-group comparison, while one-way analysis of variance (ANOVA) test was used for multiple-group comparison, using GraphPad Prism. A p value less than 0.05 was considered significantly different.

Results and discussion

Blank LPs and PTX-LPs were synthesized by the classic thin-film evaporation and hydration method. DLS revealed that the hydrodynamic diameter of LPs assembled from DOPC, Chol, and DSPE–PEG was around 135 nm with negatively charged

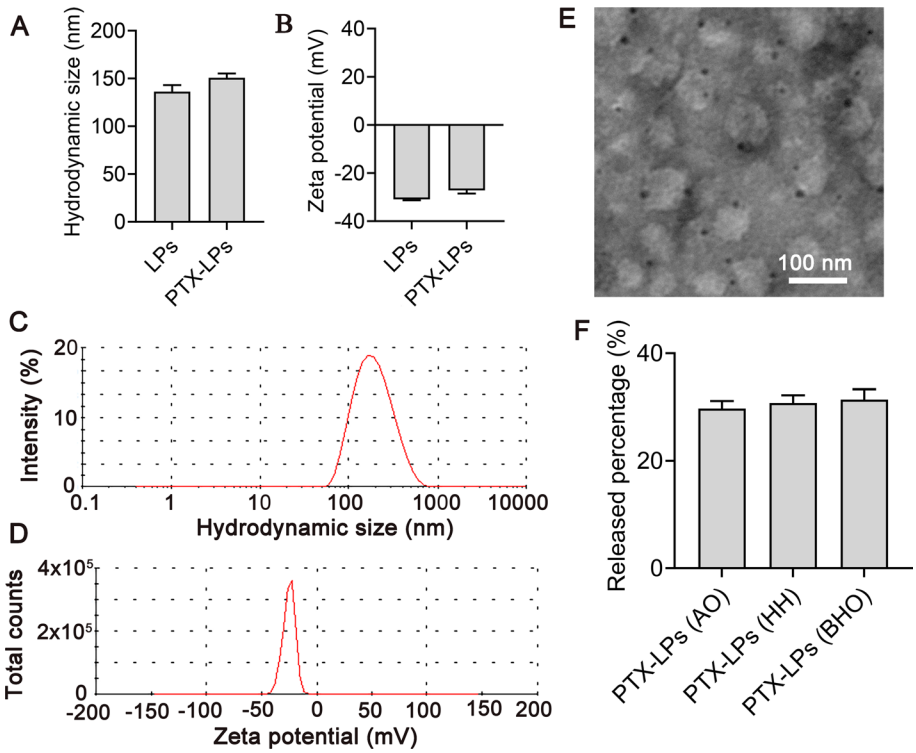

Fig. 1 LPs characterization. **A** Hydrodynamic size and (**B**) zeta potential of blank LPs and PTX-LPs. Representative curves of (**C**) hydrodynamic size and (**D**) zeta potential of PTX-LPs. **E** TEM image of PTX-LPs. **F** Release percentage of PTX-LPs after HH or HBO exposure for 1.5 h. PTX-LPs maintained under AO served as control group. Data were presented as mean ± SD ($n = 3$)

surface. After PTX loading, their diameter was slightly increased with slightly neutralized surface charge (Fig. 1A, B). The representative curves of hydrodynamic size and zeta potential of PTX-LPs are shown in Fig. 1C, D. TEM image exhibited that PTX-LPs were spherical with TEM size significantly less than hydrodynamic size (Fig. 1E). The weight ratio of fed lipids to PTX was 5:1. At this ratio, PTX-LPs had a high EE (85.1%) and LE (14.5%). Increasing fed lipids or reducing fed PTX would slightly improve EE but significantly deteriorate LE. For example, when the ratio was 10:1, EE increased to 90.3%, whereas LE sharply reduced to 8.3%. Meanwhile, although increasing fed PTX could increase LE, it was harmful to the stability of LPs, leading to rapid precipitation. In the following, in vitro drug release of PTX-LPs was investigated to determine whether HH and HBO exposure could result in the damage of liposomal membrane or structural instability of LPs for drug leakage. As demonstrated in Fig. 1F, the released percentage of PTX from PTX-LPs under HH and HBO was very similar to that maintained under AO. This result suggests that HH and HBO exposure for at least 1.5 h will not impair structural stability of LPs as well as not promoting drug release.

It is extensively reported that nanomedicines have profoundly improved pharmacokinetics compared with their corresponding free forms. Herein, despite relatively high mean plasma drug concentration of PTX-LPs compared with free PTX at 1.5 h post-injection, no considerable difference was found between them. Similar

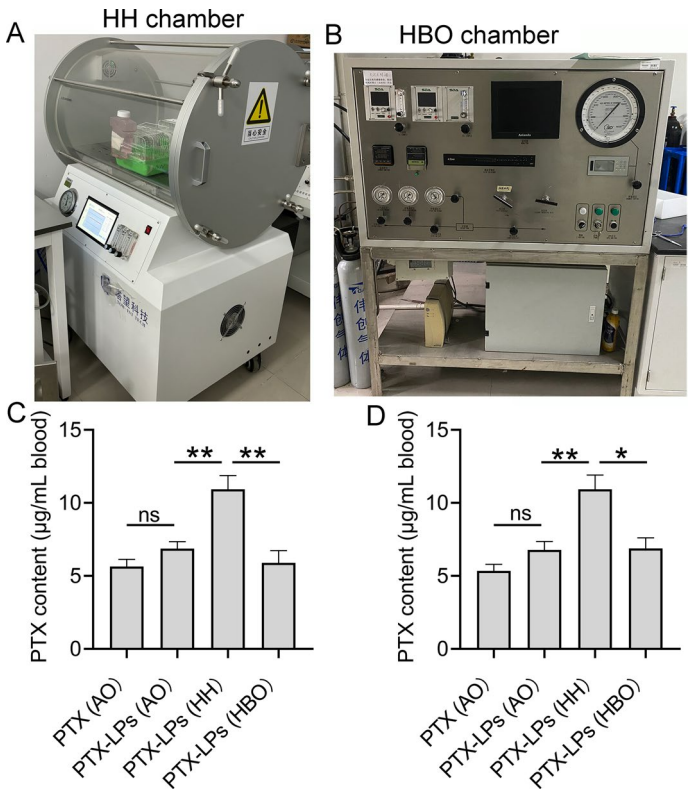

Fig. 2 Effects of HH and HBO exposure on the pharmacokinetics of PTX-LPs. Photographs of (**A**) HH and (**B**) HBO chambers. Plasma drug concentration of free PTX and PTX-LPs after (**C**) the 1st treatment and (**D**) the 2st treatment. Healthy mice were intravenously injected with free PTX and PTX-LPs (5 mg PTX/kg body weight) and immediately subjected to HH or HBO exposure for 1.5 h. Data were presented as mean ± SEM ($n = 4$). $^{*}p < 0.05$ and $^{**}p < 0.01$

phenomenon was observed in others' work (Li et al. 2011). Interestingly, HH exposure considerably improved the pharmacokinetics of PTX-LPs, while HBO exposure had no beneficial effect on the pharmacokinetics and even impaired the pharmacokinetics (Fig. 2A–C). Similar trend was observed in the repeated injection-exposure treatment regimen (Fig. 2D). It is suggested that HH would impair the activity of drug-metabolizing enzymes and therefore compromise the metabolization of drugs for the improvements in their pharmacokinetics (Vij et al. 2012; Zhu et al. 2022). Of course, HH can also upregulate the expression of some proteins to facilitate drug metabolization, which ultimately impairs pharmacokinetics (Luo et al. 2017). The results regarding the effect of HBO on pharmacokinetics of drugs are also contradictory. It was found that HBO had no considerable role in the pharmacokinetics of gentamicin (Merritt and Slade 1993), while beneficial effect was observed in carboplatin (Suzuki et al. 2008; Yamazaki et al. 2006). These results indicate that the effect of HH and HBO on pharmacokinetics of drugs including nanomedicines are very complex, which is far away from being completely understood.

In the following, the effect of HH and HBO exposure on tissue distribution of PTX-LPs was investigated. As shown in Fig. 3, HH exposure generally improved distribution of PTX-LPs in various normal tissues, especially showing significant difference in

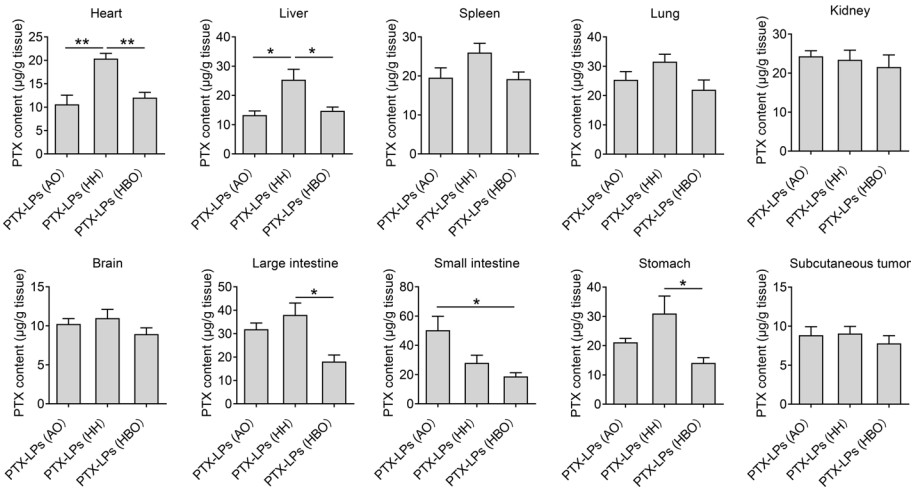

Fig. 3 Tissue distribution of PTX-LPs in the heart, liver, spleen, lung, kidney, brain, large intestine, small intestine, stomach, and subcutaneous tumor after HH and HBO exposure. Subcutaneous tumor-bearing BALB/c mice were intravenously injected with PTX-LPs (5 mg PTX/kg body weight) and immediately subjected to HH or HBO exposure for 1.5 h. Data were presented as mean ± SEM ($n = 4$). $^{*}p < 0.05$ and $^{**}p < 0.01$

the heart and liver in comparison with AO. Under AO, the vascular wall of the body is tight, which does not allow easy paracellular transport. With HH exposure, the vascular permeability increases, thus facilitating nanoparticles penetration for improved tissue distribution (Devadasu et al. 2012). Of course, improved pharmacokinetics under HH might also contribute to improved tissue distribution. This finding suggests that HH exposure might be particularly suitable to deliver heart or liver-targeted drugs. Unexpectedly, HBO exposure exerted no beneficial influence in tissue distribution of PTX-LPs in comparison with AO, and even remarkably impaired tissue distribution in the heart, liver, large intestine, and stomach compared with HH. Moreover, there was no considerable difference in the distribution of PTX-LPs in subcutaneous tumor under AO, HH, and HBO. The reason remained unclear. It has been evidenced that HBO exposure can directly improve oxygen content in major tissues as well as in tumor, and can thus facilitate drug penetration across tumor to boost chemotherapy (Wang et al. 2021). Contrary to this, adjuvant HBO exposure unfortunately exhibited no therapeutic advantage over PTX-LPs in subcutaneous tumor-bearing mice in our further animal experiment (data not shown), which accorded well with the distribution in tumor. This result suggests that the responses of cancer to HBO might be cancer type-dependent (Moen and Stuhr 2012).

The results regarding adjuvant HBO exposure in cancer therapy were disappointing. However, in views of HH-promoted distribution in the liver, it is interesting to study whether HH exposure can improve nanomedicines distribution in orthotopic liver tumor for enhanced therapy. With the protocol illustrated in Fig. 4A, the effect of HH and HBO exposure on the distribution of PTX-LPs in orthotopic liver tumor tissue was first determined. In line with our expectation, compared with AO and HBO, HH exposure significantly improved the distribution (Fig. 4B). Encouraged by this, the injection-exposure treatment was repeated and therapeutic outcome of PTX-LPs

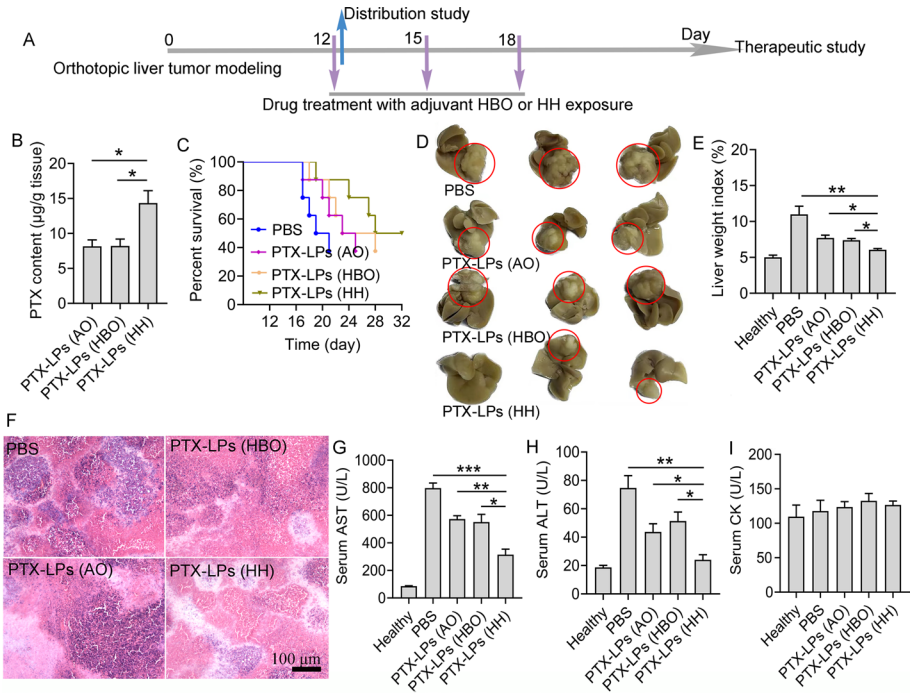

Fig. 4 Therapeutic outcome and safety evaluation in orthotopic liver tumor-bearing mice. **A** Protocol for therapeutic outcome and safety evaluation. **B** PTX content in orthotopic liver tumor after drug treatment followed by HBO or HH exposure for 1.5 h. **C** Survival monitoring. **D** Photographs of harvested tumor-bearing livers. Red circles indicated tumor sites of the livers. **E** Liver weight index. **F** H&E staining of orthotopic liver tumor. Hematologic examination for (**G**) AST and (**H**) ALT reflecting liver function. **I** Hematologic examination for CK reflecting heart function. Orthotopic liver tumor-bearing mice were intravenously injected with PTX-LPs (5 mg PTX/kg body weight) and immediately subjected to HH or HBO exposure for 1.5 h. Data were presented as mean ± SEM ($n = 3$ or 8). $^{*}p < 0.05$, $^{**}p < 0.01$, and $^{***}p < 0.001$

under AO, HH, and HBO was compared. As shown in Fig. 4C, the mean survival time of PBS, PTX-LPs (AO), PTX-LPs (HBO), and PTX-LPs (HH) was 20, 24, 25.5, and 30 days, respectively. HH exposure considerably enhanced therapeutic outcome of PTX-LPs for prolonged survival time. At the end of animal experiment, the liver with orthotopic tumor was collected for photographing and weighing. It was found that the orthotopic tumor in PTX-LPs (HH) was relatively small, contributing to remarkably low liver weight index compared with PBS, PTX-LPs (AO), and PTX-LPs (HBO) groups (Fig. 4D, E). Histopathological study by H&E staining further revealed that highly proliferative tumor cells were effectively inhibited in PTX-LPs (HH) group, leading to a large necrotic region (Fig. 4F). Hematologic result was also indicative of therapeutic outcome. As shown in Fig. 4G, H, compared with healthy mice, orthotopic liver tumor caused significant increase of serum AST and ALT serving as the indicators of liver function. After treatment with PTX-LPs (AO) and PTX-LPs (HBO), AST and ALT decreased, due to the inhibition of orthotopic liver tumor. Especially, PTX-LPs (HH) treatment further notably decreased AST and ALT, indicating their enhanced therapeutic outcome compared with PTX-LPs (AO) and PTX-LPs (HBO). According to the treatment protocol, the mice were subjected to intermittent HH after drug treatment. While intermittent HH is not supposed to be of anti-tumor

outcome, the enhanced therapeutic outcome of PTX-LPs (HH) is owing to HH-promoted distribution of PTX-LPs in the liver for facilitated accumulation in tumor.

Given that HH also improved the distribution of PTX-LPs in the heart, the cardiotoxicity caused therefrom was a serious concern. Fortunately, no difference in serum CK reflecting heart function was found between healthy group and tumor-bearing mice with or without the treatment. There was also no difference in body weight among all groups (data not shown). These results suggest that HH exposure itself is safe to the heart. Moreover, despite HH-promoted substantial distribution of PTX-LPs in the heart, the reduced toxicity of PTX-nanomedicine ensures the safety of PTX-LPs treatment with adjuvant HH exposure.

Conclusion

In summary, we prepared PTX-LPs and then studied the effect of HH and HBO exposure on their pharmacokinetics and tissue distribution. The results showed that HH exposure significantly improved the pharmacokinetics of PTX-LPs with facilitated distribution in the heart and liver, whereas HBO did not benefit and even impaired the pharmacokinetics and distribution. Given that HH exposure could not improve the distribution in subcutaneous tumor, we thus constructed orthotopic liver tumor model, with the aim to improve therapeutic outcome of PTX-LPs in treating liver cancer through HH-promoted distribution in the liver for further effective accumulation in tumor. As expected, PTX-LPs with adjuvant HH exposure significantly inhibited the growth of orthotopic liver tumor for prolonged survival time, while not causing unfavorable side effect. Our finding revealed the potential of intermittent HH exposure in treating liver cancer.

Abbreviations

ALT	Alanine aminotransferase
AO	Atmospheric oxygen
AST	Aspartate aminotransferase
ATA	Atmosphere absolute
Chol	Cholesterol
CK	Creatine kinase
DLS	Dynamic light scattering
DOPC	1,2-Dioleoyl-sn-glycero-3-phosphocholine
DSPE–PEG	1,2-Distearoylsn-glycero-3-phosphoethanolamine-N-[methoxy (polyethylene glycol)-2000
EE	Encapsulation efficiency, %
EPR	Enhanced permeability and retention effect
HBO	Hyperbaric oxygen
H&E	Hematoxylin and eosin
HH	Hypobaric hypoxia
HPLC	High-performance liquid chromatography
LE	Loading efficiency, %
LPs	Liposomes
PTX	Paclitaxel
PTX-LPs	PTX-loaded liposomes
TEM	Transmission election microscope
TME	Tumor microenvironment

Author contributions

YT carried out the experiments; ZC designed the experiments and wrote the manuscript.

Funding

The work was supported by the Open Research Fund of State Key Laboratory of Bioelectronics, Southeast University (OPSKLB202007).

Availability of data and materials

Data and materials are available from the corresponding author on reasonable request.

Declarations

Ethics approval and consent to participate
No human participants, human data or human tissue were involved in this study. All animal experiments were carried out in accordance with the protocols approved by Animal Care and Use Committee of Nantong University.

Consent for publication
All authors read and approved the final version of the manuscript.

Competing interests
The authors declared no conflict of interest.

Received: 23 January 2024 Accepted: 27 March 2024
Published online: 02 April 2024

References

Anand U, Dey A, Chandel AKS, Sanyal R, Mishra A, Pandey DK, De Falco V, Upadhyay A, Kandimalla R, Chaudhary A, Dhanjal JK, Dewanjee S, Vallamkondu J, Pérez de la Lastra JM (2023) Cancer chemotherapy and beyond: current status, drug candidates, associated risks and progress in targeted therapeutics. Genes & Diseases 10:1367–1401

Behranvand N, Nasri F, Zolfaghari Emameh R, Khani P, Hosseini A, Garssen J, Falak R (2022) Chemotherapy: a double-edged sword in cancer treatment. Cancer Immunol Immunother 71:507–526

Bhatia SN, Chen X, Dobrovolskaia MA, Lammers T (2022) Cancer nanomedicine. Nat Rev Cancer 22:550–556

Burtscher M, Millet GP, Burtscher J (2022) Hypoxia conditioning for high-altitude pre-acclimatization. J Sci Sport Exer 4:1–15

Cai XL, Jin M, Yao LFK, He B, Ahmed S, Safdar W, Ahmad I, Cheng DB, Lei ZX, Sun TL (2023) Physicochemical properties, pharmacokinetics, toxicology and application of nanocarriers. J Mater Chem B 11:716–733

Cao MX, Long MM, Chen QP, Lu YP, Luo QQ, Zhao Y, Lu AL, Ge CW, Zhu L, Chen ZP (2019) Development of -elemene and cisplatin co-loaded liposomes for effective lung cancer therapy and evaluation in patient-derived tumor xenografts. Pharm Res 36:121

Chen Q, Yuan L, Chou W-C, Cheng Y-H, He C, Monteiro-Riviere NA, Riviere JE, Lin Z (2023) Meta-analysis of nanoparticle distribution in tumors and major organs in tumor-bearing mice. ACS Nano 17:19810–19831

Devadasu VR, Wadsworth RM, Ravi Kumar MNV (2012) Tissue localization of nanoparticles is altered due to hypoxia resulting in poor efficacy of curcumin nanoparticles in pulmonary hypertension. Eur J Pharm Biopharm 80:578–584

He C, Hu Y, Yin L, Tang C, Yin C (2010) Effects of particle size and surface charge on cellular uptake and biodistribution of polymeric nanoparticles. Biomaterials 31:3657–3666

Li R, Eun JS, Lee M-K (2011) Pharmacokinetics and biodistribution of paclitaxel loaded in pegylated solid lipid nanoparticles after intravenous administration. Arch Pharm Res 34:331–337

Liu X, Ye N, Xiao C, Wang X, Li S, Deng Y, Yang X, Li Z, Yang X (2021) Hyperbaric oxygen regulates tumor microenvironment and boosts commercialized nanomedicine delivery for potent eradication of cancer stem-like cells. Nano Today 40:101248

Liu XM, Sun JJ, Gu J, Weng LY, Wang XT, Zhu L, Luo QQ, Chen ZP (2023) Effective drug and shRNA delivery for synergistic treatment of triple-negative breast cancer by sequentially targeting tumor hypoxia. Chem Eng J 470:144271

Long MM, Lu AL, Lu M, Weng LY, Chen QP, Zhu L, Chen ZP (2020) Azo-inserted responsive hybrid liposomes for hypoxia-specific drug delivery. Acta Biomater 115:343–357

Long MM, Liu XM, Huang XL, Lu M, Wu XM, Weng LY, Chen QP, Wang XT, Zhu L, Chen ZP (2021) Alendronate-functionalized hypoxia-responsive polymeric micelles for targeted therapy of bone metastatic prostate cancer. J Control Release 334:303–317

Lu M, Huang X, Cai X, Sun J, Liu X, Weng L, Zhu L, Luo Q, Chen Z (2022) Hypoxia-responsive stereocomplex polymeric micelles with improved drug loading inhibit breast cancer metastasis in an orthotopic murine model. Acs Appl Mater Inter 14:20551–20565

Luo B, Wang R, Li W, Yang T, Wang C, Lu H, Zhao A, Zhang J, Jia Z (2017) Pharmacokinetic changes of norfloxacin based on expression of MRP2 after acute exposure to high altitude at 4300 m. Biomed Pharmacother 89:1078–1085

Merritt GJ, Slade JB (1993) Influence of hyperbaric oxygen on the pharmacokinetics of single-dose gentamicin in healthy volunteers. Pharmacotherapy 13:382–385

Moen I, Stuhr LE (2012) Hyperbaric oxygen therapy and cancer—a review. Target Oncol 7:233–242

Subhan MA, Parveen F, Filipczak N, Yalamarty SSK, Torchilin VP (2023) Approaches to improve EPR-based drug delivery for cancer therapy and diagnosis. J Pers Med 13:389

Sun D, Gao W, Hu H, Zhou S (2022a) Why 90% of clinical drug development fails and how to improve it? Acta Pharm Sin B 12:3049–3062

Sun R, Xiang J, Zhou Q, Piao Y, Tang J, Shao S, Zhou Z, Bae YH, Shen Y (2022b) The tumor EPR effect for cancer drug delivery: current status, limitations, and alternatives. Adv Drug Del Rev 191:114614

Suzuki Y, Tanaka K, Neghishi D, Shimizu M, Murayama N, Hashimoto T, Yamazaki H (2008) Increased distribution of carboplatin, an anti-cancer agent, to rat brains with the aid of hyperbaric oxygenation. Xenobiotica 38:1471–1475

Vij AG, Kishore K, Dey J (2012) Effect of intermittent hypobaric hypoxia on efficacy & clearance of drugs. Indian J Med Res 135:211–216

Wang FF, Chen L, Zhang R, Chen ZP, Zhu L (2014) RGD peptide conjugated liposomal drug delivery system for enhance therapeutic efficacy in treating bone metastasis from prostate cancer. J Control Release 196:222–233

Wang P, Wang X-Y, Man C-F, Gong D-D, Fan Y (2023) Advances in hyperbaric oxygen to promote immunotherapy through modulation of the tumor microenvironment. Front Oncol 13:1200619

Wang X, Li S, Liu X, Wu X, Ye N, Yang X, Li Z (2021). Boosting Nanomedicine Efficacy with Hyperbaric Oxygen Therapy. Bio-Nanomed Cancer Therapy. pp. 77–95
Wu X, Zhu Y, Huang W, Li J, Zhang B, Li Z, Yang X (2018) Hyperbaric oxygen potentiates doxil antitumor efficacy by promoting tumor penetration and sensitizing cancer cells. Adv Sci 5:1700859
Yamazaki H, Tanaka K, Gamura S, Hashimoto T, Shimizu M (2006) High-performance Liquid chromatographic assay for carboplatin in ultrafiltered plasma combined with hyperbaric oxygenation. Drug Metab Pharmacokinet 21:429–431
Yang Y, Xie X, Yang Y, Zhang H, Mei X (2013) A review on the influences of size and surface charge of liposome on its targeted drug delivery in vivo. Acta Pharmaceutica Sinica 48:1644–1650
Zhang P, Xiao Y, Sun X, Lin X, Koo S, Yaremenko AV, Qin D, Kong N, Farokhzad OC, Tao W (2023) Cancer nanomedicine toward clinical translation: obstacles, opportunities, and future prospects. Med 4:147–167
Zhu J, Duan Y, Duo D, Yang J, Bai X, Liu G, Wang Q, Wang X, Qu N, Zhou Y (2022) High-altitude hypoxia influences the activities of the drug-metabolizing enzyme CYP3A1 and the pharmacokinetics of four cardiovascular system drugs. Pharmaceuticals 15:1303
Zi Y, Yang K, He J, Wu Z, Liu J, Zhang W (2022) Strategies to enhance drug delivery to solid tumors by harnessing the EPR effects and alternative targeting mechanisms. Adv Drug Del Rev 188:114449

Publisher's Note